

Geologica Acta: an international earth science journal

ISSN: 1695-6133

geologica-acta@ictja.csic.es

Universitat de Barcelona España

# MONTERO, P.; TALAVERA, C.; BEA, F.

Geochemical, isotopic, and zircon (U-Pb, O, Hf isotopes) evidence for the magmatic sources of the volcano-plutonic Ollo de Sapo Formation, Central Iberia Geologica Acta: an international earth science journal, vol. 15, núm. 4, diciembre, 2017, pp. 245-260

Universitat de Barcelona Barcelona, España

Available in: http://www.redalyc.org/articulo.oa?id=50553843002



Complete issue

More information about this article

Journal's homepage in redalyc.org



Scientific Information System

Network of Scientific Journals from Latin America, the Caribbean, Spain and Portugal Non-profit academic project, developed under the open access initiative

# Geochemical, isotopic, and zircon (U-Pb, O, Hf isotopes) evidence for the magmatic sources of the volcano-plutonic Ollo de Sapo Formation, Central Iberia

P. MONTERO1 C. TALAVERA2 F. BEA1\*

#### <sup>1</sup>Department of Mineralogy and Petrology, University of Granada

Campus Fuentenueva, 18002 Granada, Spain. F. Bea E-mail: fbea@ugr.es; phone +34 958246176; fax: +34 958 243358

<sup>2</sup>John de Laeter Centre, Curtin University Perth, Western Australia 6102, Australia

\*Corresponding author

## $\dashv$ ABSTRACT $\vdash$

The Ollo de Sapo Formation comprises variably metamorphosed felsic peraluminous volcanic rocks and high-level granites that crop out over some 600km from the Cantabrian coast to central Spain in the northern part of the Central Iberian Zone. The Ollo de Sapo magmatism is not obviously connected with any major tectonic or metamorphic event so its origin is controversial. Some authors, based on trace-elements, have proposed that the Ollo de Sapo magmas originated in a supra-subduction setting but others, based on abnormally high zircon inheritance and field and structural data, favored a rifting environment. Here we present new oxygen and hafnium isotope data from the very characteristic Ollo the Sapo zircons, which in most cases, consist of ca. 485Ma rims and ca. 590-615Ma cores. We found that the Cambrian-Ordovician rims yielded unimodal distributions that cluster around  $\partial^{18}O = 10$ , typical of S-type magmas formed from melting of altered crust. The Ediacaran cores, in contrast, cluster around  $\partial^{18}O = 6.5$ , consistent with being arc-magmas. Rims and cores have the same average Hf isotope composition, but the rims are considerably more uniform. These data, coupled with existing whole-rock element and Sr and Nd isotopic data, indicate that the Ollo de Sapo were S-type magmas that resulted from anatexis of younger-than-600Ma immature sediments mostly derived from different Ediacaran igneous rocks with a wide range of Hf isotope composition.

KEYWORDS

SHRIMP. Isotopes. Extension. Gneisses. Magmatic source.

# INTRODUCTION

The Ollo de Sapo (Toad's Eye) Formation is the largest accumulation of Cambrian-Ordovician magmatic rocks in the Iberian Massif. It comprises variably metamorphosed felsic peraluminous volcanic rocks and high-level granites. The Formation crops out in the core of

a Variscan anticlinorium extending for about 600km from the Cantabrian coast to central Spain in the northern part of the Central Iberian Zone (Fig. 1; Parga-Pondal *et al.*, 1964; Díez Montes *et al.*, 2004, and references therein). Rocks of similar composition, structure, and age are also found in other localities: i) forming a batholithic complex in the Eastern part of the Spanish Central System (Vialette

et al., 1987; Wildberg et al., 1989; Talavera et al., 2013), ii) scattered in the anatectic complexes of the Central Iberian Zone (Bea et al., 2003; Talavera et al., 2013), and iii) forming the Urra Formation at the southern boundary of the Central Iberian Zone with the Ossa Morena Zone (Fig. 1; Sola et al., 2008, and references therein).

The Ollo de Sapo gneisses have two notable characteristics. First, they are not obviously connected with any major tectonic or metamorphic event (Gutiérrez Marco *et al.*, 2002). Second, they have an unusually high proportion of inherited zircons: in the 20 massifs we have

studied so far, no less than 70-80%, and in some samples nearer 100%, of zircon grains contain pre-magmatic cores (Bea *et al.*, 2006b; Montero *et al.*, 2007; Montero *et al.*, 2009; Talavera *et al.*, 2013). This high degree of inheritance seems to be a common feature of the Cambrian-Ordovician rocks of Western Europe (*e.g.* Laumonier *et al.*, 2004; Teipel *et al.*, 2004; Helbing and Tiepolo, 2005) that undoubtedly reflects a fundamental fact of their formation.

The whole-rock geochemistry of the Ollo de Sapo gneisses is felsic, markedly peraluminous and alkaline-calcic —in the Frost *et al.* (2001) rather than in the

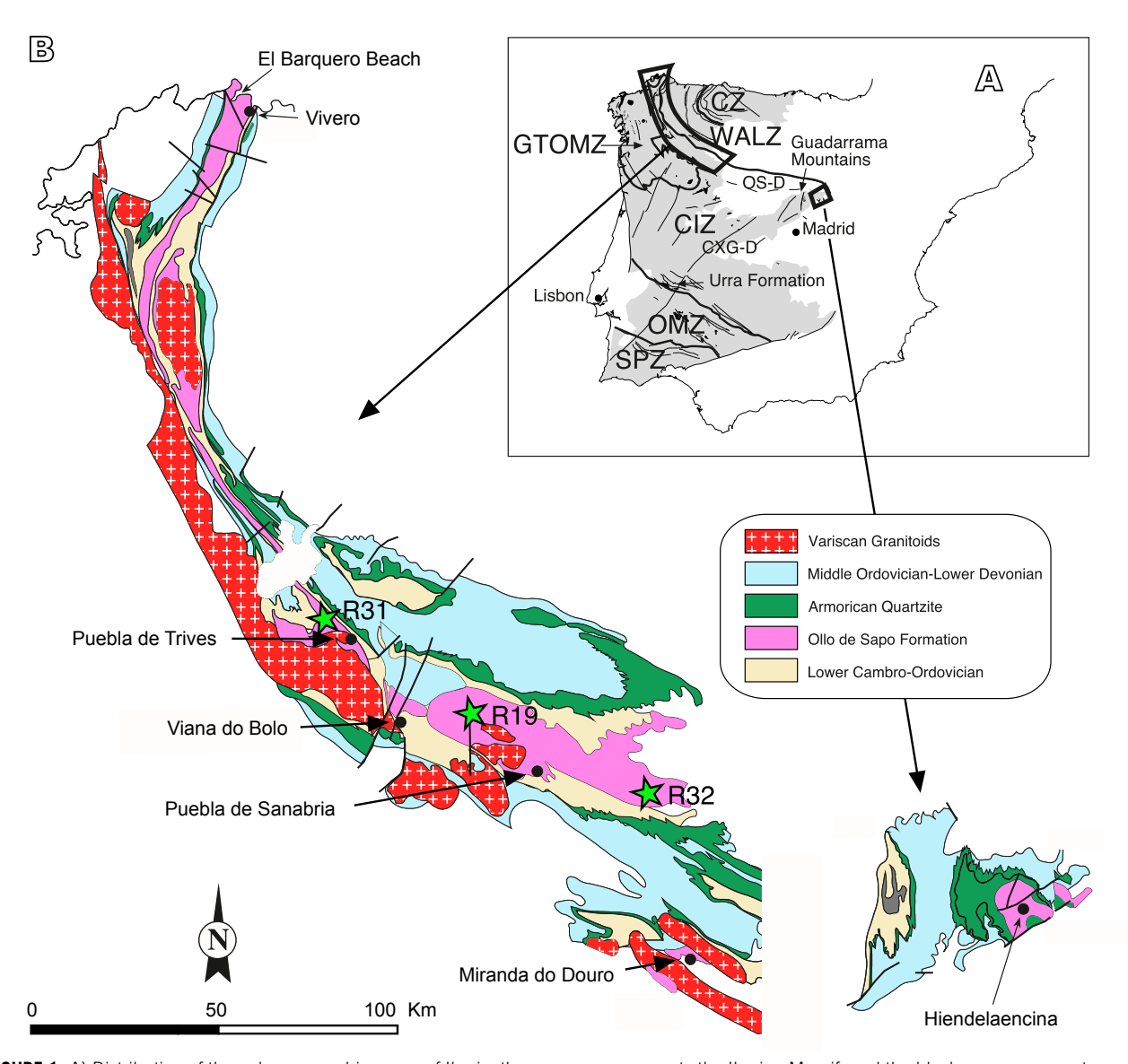


**FIGURE 1.** A) Distribution of the paleogeographic zones of Iberia; the gray area represents the Iberian Massif, and the black areas represent exposures of Cambrian-Ordovician rocks. CIZ = Central Iberian Zone; CXG-D = Schist-Graywacke Complex Domain; CZ = Cantabric Zone; GTOMZ = Galicia Trás os Montes Zone; OMZ = Ossa Morena Zone; OS-D = Ollo de Sapo Domain; SPZ = South Portuguese Zone; and WALZ = Western-Asturian Leonian Zone. B) The Ollo de Sapo Anticlinorium. Stars represent the three samples studied for zircon oxygen and hafnium isotopes. Their composition is given in Table 1.

Peacock (1931) sense— with trace element features that bear similarities with those shown by arc magmas (see below). Based on this, and despite the lack of petrological or regional evidence, some authors have proposed that the Ollo de Sapo magmas originated in a supra-subduction setting (e.g. Gebauer et al., 1993; Valverde-Vaquero and Dunning, 2000; Navidad and Bea, 2004; Del Greco et al., 2016). Other authors, however, disagreed and favored a rifting environment. Bea et al. (2007) for example, based on the abnormally high zircon inheritance, proposed that the Ollo de Sapo magmas resulted from extremely fast melting rates in the middle-lower crust followed by fast melt transportation to the upper crust in an extensional regime. Díez Montes et al. (2010) reached analogous conclusions based on field and structural data.

It is evident that the controversies about the petrogenesis and geodynamic significance of the Ollo de Sapo gneisses mainly arise from the lack of understanding of the nature of the magmas involved. This paper attempts to identify the magmatic sources which, we believe, is the first step in that direction. To this end we combined the inferences derived from exploitation of a large dataset of whole-rock element and Sr and Nd isotopes obtained by the authors over the years, with new oxygen and hafnium isotope data from the very characteristic Ollo the Sapo zircons. The results indicate that the Ollo de Sapo magmas derived from immature sediments of Late Ediacaran to Cambrian age and are, therefore, S-type felsic magmas generated in an extensional environment.

#### **GEOLOGICAL SETTING AND PETROGRAPHY**

The Ollo de Sapo Formation crops out in the core of a Variscan anticlinorium extending for about 600km from the west Cantabrian Coast to central Spain (Fig. 1; see an overview in Díez Montes *et al.*, 2004). It consists of metavolcanic and metagranitic rocks that are overlain by a clastic succession topped by the Armorican Quartzite, and underlain by another succession of Early to Middle Cambrian rocks that were locally highly metamorphosed (Díez Montes *et al.*, 2010).

The metavolcanic rocks, which originally consisted of dacitic to rhyolitic ignimbrites and tuffs, are currently represented by augen-gneisses with large, and locally rapakivi, megacrysts of K-feldspar, within a fine- to medium-grained and strongly foliated felsic peraluminous groundmass. These gneisses may be grouped into two facies, one coarse-grained and the other fine-grained. The coarse-grained facies usually crops out in the lower part of the formation. It is mainly composed of K-feldspar megacrysts (up to 15cm) and plagioclase and quartz phenocrysts (up to 3cm) embedded in a fine-grained

groundmass that, in most cases, consists of quartz, K-feldspar, muscovite, biotite, rare albite, chlorite and sericite, with apatite, zircon, monazite, xenotime, ilmenite and Fe-Cu sulfides as accessories. The fine-grained facies is commonly found in the upper part of the formation and consists of small phenocrysts of K-feldspar (up to 2cm) and quartz (up to 1.5-2cm) in a fine-grained matrix similar to the groundmass of the coarse-grained facies.

The metagranites, which originally consisted of high-level granites, are currently represented by coarse-grained augen-gneisses with intrusive contacts and recognizable aplopegmatitic dykes and enclaves. They crop out as sills or laccoliths in the cores of large antiforms and intruding the Early to Middle Cambrian sequences underlying the Ollo de Sapo (González Lodeiro, 1981; Iglesias Ponce de Leon and Ribeiro, 1981; Díez Montes *et al.*, 2010). The metagranites are composed of large K-feldspar megacrysts embedded in a coarse-grained groundmass of quartz, plagioclase, K-feldspar, biotite, muscovite that may be accompanied of rare tourmaline, cordierite and garnet. The accessories assemblage consists of apatite, zircon, monazite, rare xenotime and Fe-Ti oxides.

#### SAMPLES AND METHODS

For this work we have used 32 samples collected all throughout the Ollo de Sapo Formation. All samples were analyzed for major and trace elements, and 28 of them were also analyzed for Sr and Nd isotopes. To avoid inter-laboratory effects all analyses, except Hf isotopes, have been undertaken in the authors' laboratories at the Centro de Instrumentación Científica of the University of Granada (CIC-UGR). Zircons from 11 samples have been dated previously using single-grain evaporation and SIMS techniques (Montero et al., 2007; 2009; Talavera et al., 2013). For this work we have separated zircons from three new samples representing the most common facies of the Ollo de Sapo rocks: one metagranite (R19) and two metavolcanic rocks, one coarse-grained (R32) and the other fine-grained (R31; Fig. 1). Using the SHRIMP, we dated them and determined their oxygen isotope composition. Hf isotopes were determined using a MC-LA-ICPMS system.

Whole-rock major-element and Zr determinations were done by XRF after fusion with lithium tetraborate. Typical precision was better than  $\pm 1.5\%$  for an analyte concentration of 10 wt.%. Trace-element determinations, except Zr, were done by ICP-MS using Rh as an internal standard. Samples were dissolved in HNO<sub>3</sub> + HF at a pressure of 180p.s.i. in a microwave digestor, dried and redissolved in 4% HNO<sub>3</sub>. Precision, estimated from the analyses of 10 replicates of one sample, was better

than  $\pm 2\%$  and  $\pm 5\%$  for analyte concentrations of 50 and 5ppm respectively.

Samples for Sr and Nd isotope studies were digested in a clean room using ultra-clean reagents and analyzed by TIMS in a Finnigan Mat 262 spectrometer after chromatographic separation with ion-exchange resins. Normalization values were 86Sr/88Sr=0.1194 and <sup>146</sup>Nd/<sup>144</sup>Nd=0.7219. Blanks were 0.6 and 0.09ng for Sr and Nd, respectively. The external precision  $(2\sigma)$ , estimated from the results of the last 10 replicates of the standard WS-E (Govindaraju et al., 1994), which is routinely analyzed each 10 unknown samples, was better than 0.003% for <sup>87</sup>Sr/<sup>86</sup>Sr, and 0.0015% for <sup>143</sup>Nd/<sup>144</sup>Nd. <sup>87</sup>Rb/<sup>86</sup>Sr and <sup>147</sup>Sm/<sup>144</sup>Nd were directly determined by ICP-MS (Montero and Bea, 1998) with a precision, estimated by analyzing 10 replicates of the standard WS-E, better than 1.2% and 0.9%  $(2\sigma)$ , respectively.

Zircon was separated using panning, first in water and then in ethanol. After eliminating the magnetic fraction from the concentrates with a neodymium magnet, zircons were handpicked under a binocular microscope and put in a SHRIMP megamount (Ickert et al., 2008). Once mounted and polished, zircon grains were studied by optical and cathodoluminescent imaging, coated with a 10nm thick gold layer, and analyzed for U-Th-Pb and Oxygen isotopes using a SHRIMP IIe/mc ion microprobe at the IBERSIMS laboratory of the Centro de Instrumentación Científica of the University of Granada (CIC-UGR). The SHRIMP U-Th-Pb analytical method roughly followed the described by Williams and Claesson (1987), and is described in detail in www.ugr.es/ibersims. Uranium concentration was calibrated using the SL13 reference zircon (U: 238ppm). U/Pb ratios were calibrated using the TEMORA-II reference zircon (417Ma; Black et al., 2003) which was measured every 4 unknowns. When required, common lead was corrected from the measured 204Pb/206Pb, using the model of terrestrial Pb evolution of Cumming and Richards (1975). Pointto-point errors (95% C.I.) on the age standard were  $\pm 0.23\%$  for  $^{206}\text{Pb}/^{238}\text{U}$  and  $\pm 0.46\%$  for  $^{207}\text{Pb}/^{206}\text{Pb}$ . Data reduction was done with the SHRIMPTOOLS software (downloadable from www.ugr.es/~fbea) using the STATA<sup>TM</sup> programming language.

Once analyzed for U-Th-Pb, the megamounts were cleaned, re-polished, and coated with a 30nm thick gold layer for oxygen isotope analyses. To this end the SHRIMP primary ion optics was set with a  $120\mu m$  Kohler aperture to produce a  $\sim 18\mu m$  diameter spot on the mount surface. The Cs gun was set to yield a  $\sim 8nA$  Cs+ beam. The e-gun to neutralize Cs ions on non-conductive

materials was set to an intensity of about 1µA. Spots to be analyzed were burned for about 5 minutes before measurements. During this time the secondary beam and the e-gun were fully optimized to maximize the <sup>16</sup>O signal. Measurements were done in two sets of 10 scans each. The scans were of 10 seconds each so that the real data collection time was 200 seconds per spot. The EISIE (electron induced secondary ion emission) background was recorded during 10s before and after each set, and subtracted from the <sup>18</sup>O and <sup>16</sup>O counts. As a standard we used the TEMORA-II zircon measured every four unknowns and cross-checked again the 91500 zircon every 20 unknowns. The reproducibility of the standards was excellent:  $\partial^{18}O=8.17\pm0.34$  (2s) for the TEMORA-II and  $\partial^{18}O=9.98\pm0.26$  (2s) for the 91500, respectively. Data reduction was done with the POXY program developed by P. Lanc and P. Holden at the Australian National University.

Hf isotopes were done at the Geochronology and Isotope Geochemistry-SGIker facility of the University of the Basque Country using a Thermo-Fisher Scientific Neptune MC-ICP-MS coupled to the New Wave Research UP-213 laser system with a SuperCell laser cell. Data were collected in static mode during 50s of ablation with a spot size of 40 µm. Masses 171, 173, and 175 were simultaneously monitored during each step to correct the isobaric interferences of Lu and Yb isotopes on mass 176. <sup>176</sup>Yb and <sup>176</sup>Lu were calculated assuming a <sup>176</sup>Yb/<sup>173</sup>Yb of 0.796179 and a 176Lu/175Lu of 0.02655 (Chu et al., 2002) and taking into account the instrumental mass fractionation of each individual analysis. To correct Instrumental Mass Fractionation (IMF) Yb isotope ratios were normalized to  $^{173}$ Yb/ $^{171}$ Yb=1.132685 and Hf isotope ratios to  $^{179}$ Hf/ $^{177}$ Hf to 0.7325 (ibid.) using an exponential law. The Lu IMF was assumed to follow that of Yb. Data reduction was performed using the Iolite 2.5 software package for deconvolution of time resolved data (Paton et al., 2011).

#### **GEOCHEMICAL AND ISOTOPIC SIGNATURES**

The major element compositions of the Ollo de Sapo gneisses (Table 1) correspond to variably silicic granitoids that are magnesian (Fig. 2A), alkaline-calcic to calc-alkaline (Fig. 2B) and markedly peraluminous: the aluminum saturation index (ASI=mol. Al<sub>2</sub>O<sub>3</sub>/(CaO+Na<sub>2</sub>O+K<sub>2</sub>O)) varies from 1.16 to 2.07 with the most common values around 1.4 (Fig. 3). The proportions of normative feldspars correspond to granites *sensu stricto* (Fig. 4A) and the proportions of normative albite, orthoclase and quartz are identical to ordinary corundum-normative (peraluminous) granites (Fig. 4B). We have found no meaningful compositional differences between metavolcanic and metaplutonic facies.

TABLE 1. Major and trace elements of the Ollo de Sapo gneisses. See text

-	R01	R02	R03	R04	R05	R06	R07	R08	R09	R10	R11	R12	R13	R14	R15	R16
SiO <sub>2</sub>	68.06	63.44	65.61	68.83	69.71	66.9	69.98	66.53	66.47	64.94	66.8	66.33	68.54	66.7	66.19	67.86
TiO <sub>2</sub>	0.5	0.9	0.61	0.56	0.5	0.58	0.46	0.61	0.74	0.71	0.56	0.61	0.39	0.62	0.59	0.51
Al <sub>a</sub> O <sub>a</sub>	15.76	17.11	17.51	15.62	15.15	16.67	15.35	16.13	15.74	16.18	15.8	15.43	16.02	15.25	16.47	16.27
FeO	3.32	6.07	5.16	4.05	3.44	3.91	2.97	3.61	3.68	4.09	3.3	3.35	2.56	3.53	3.52	2.85
MgO	1.49	2.38	1.87	1.47	1.24	1.53	1.13	1.63	1.91	1.89	1.7	1.73	1.02	1.79	1.66	1.63
MnO CaO	0.04 1.38	0.08 1.6	0.09 1.02	0.06 1.08	0.05 0.95	0.06 1.12	0.05 0.87	0.04 0.37	0.05 1.16	0.05 0.67	0.04 1.38	0.05 1.4	0.04 0.5	0.05 1.23	0.05 1.05	0.04 0.69
Na <sub>2</sub> O	2.73	1.86	1.45	1.00	2.39	2.33	2.68	2.73	2.42	2.64	2.86	2.74	2.96	2.85	2.87	2.13
K20	4.18	3.08	3.9	3.77	4.15	4.49	4.42	4.95	4.09	4.21	4.18	4.36	5.18	4.31	5.12	5.26
$P_2O_5$	0.18	0.16	0.132	0.19	0.18	0.21	0.22	0.23	0.21	0.23	0.23	0.23	0.26	0.23	0.23	0.21
LOI	1.86	2.81	1.55	1.78	2.01	1.73	1.79	1.55	2.75	3.34	2.68	2.76	1.85	3.32	1.57	1.89
Total	99.51	99.49	98.91	99.12	99.77	99.53	99.92	98.39	99.22	98.95	99.53	98.99	99.32	99.88	99.32	99.34
Li	42	140	132	86	77	104	115	73	67	64	56	62	55	59	89	57
Rb Cs	159 4.9	195 12.6	173 18.9	188 11.2	146 13.5	177 16.6	241 17.8	170 7	160 7.8	141 4.9	143 6.5	145 5.9	248 8.5	152 6.7	186 9.1	197 5
Be	2.2	2.7	14.1	3.5	2.5	5.4	2	2.4	2.8	2.7	2.2	2.9	1.7	2.7	2.9	2.9
Sr	136	144	160	108	70	99	83	46	147	63	157	141	75	138	144	112
Ва	712	431	783	504	562	868	429	851	655	693	763	800	479	766	908	820
Sc	7.1	15.4	11.9	9	7.6	9.6	7.3	10.3	12.9	12.3	9.8	10.5	7.5	10.3	9.6	8.8
V Cr	61.3 57.1	101.3 85.6	77.7 60.4	60.1 40.3	55.2 39.8	65.4 48	44.9 36	67.2 53.8	82.2 63.7	78.7 59.7	66.3 49.5	69 57.2	41.3 33.9	67.2 53.5	58.6 46.8	57.5 51.8
Co	127.7	37.8	52.7	48.2	34.3	22.8	79.1	25.1	57.5	26.5	29.4	27.9	76.8	27.4	40.1	31.0
Ni	16.4	41.9	31.5	22.2	13.1	15.3	14.2	20	16.5	27.3	17.1	22.7	11.6	20.5	17.2	15.7
Cu	6.7	12.5	39.7	16.1	17.8	24.2	12.9	16	11.5	25.9	12.6	20.8	14.8	19.8	10.9	1.4
Zn	41.5	88	79.8	70	77.6	128	64.5	44.4	66.6	65.9	46.8	48.8	58.4	52	78.3	45.8
Ga Y	20 28.2	21.5 11.2	20.8 8.7	21.8 17.4	19.6 12.1	20.8 12.6	19.4 13.7	21.2 25.7	20.6 20.5	21.2 22.2	20.8 27.4	21.1 29.7	20.4 14.1	20.5 34.6	21.7 18.5	23.8 15
Nb	10.5	16.4	13	11.9	11.1	11.7	10.8	10.9	12.2	11.5	10.3	11.1	11.2	10.9	11.1	10.8
Ta	1.1	1.5	1.2	1.1	1.1	1	1.4	0.9	1.1	1	0.9	1	1.9	1	1	1.1
Zr	162	191	114	198	171	193	142	209	225	213	183	197	136	191	196	187
Hf	5.2	5.5	3.1	6.2	4.5	5.9	4.5	6.3	7.4	6.3	5.6	6	4.4	6	6.3	5.9
Mo Sn	0.6 4.1	0.5 5.3	0.2 5.2	0.5 5.4	0.3 6.6	0.3 6.8	0.4 7.1	0.7 5.1	0.4 6	0.8 4.1	0.9 4.6	0.8 4.5	0.2 15.9	0.7 4.5	0.4 5.5	0.2 6.8
TI	0.92	1.18	0.91	1.06	1.1	1.22	1.52	0.97	0.83	0.8	0.76	0.75	1.4	0.83	1.13	1
Pb	22.1	21.3	28.1	20	28	51.6	23.7	23.2	34.5	22.1	18.8	23.2	24.7	20.7	29.5	17.3
U	3.42	3.55	3.32	3.94	3.91	3.29	7.15	3.84	2.8	3.61	3.12	3.45	4.25	3.48	2.93	3.52
Th	11.15	14.77	12.44	16.56	12.56	11.94	10.89	13.03	13.85	13.58	9.83	11.84	9.99	11.55	13.98	14.18
La Ce	26.8 58.7	39.7 78.6	35.4 69.8	38.2 79	27.7 58.6	30.4 62.3	25.9 54	28.2 60.5	42.1 86.8	28.4 72.9	27.6 65.4	30.6 65.6	22.9 47.9	30.7 66.5	31.8 68.4	32.5 67.6
Pr	7.04	8.86	8.05	9.4	7.05	7.49	6.79	7.66	10.61	7.53	7.16	7.97	5.99	7.82	8.16	8.39
Nd	26.5	34.2	29.9	36.1	26.7	28.7	25.7	29	40.9	29.3	27.4	30.5	22.6	30.2	30.5	30.8
Sm	6.00	6.72	5.43	7.48	5.65	6.03	5.29	6.33	8.58	6.09	5.92	6.6	4.85	6.5	6.9	6.52
Eu	1.22	1.54	1.37	1.01	0.93	1.3	0.79	1.13	1.48	1.13	1.04	1.16	0.81	1.13	1.24	1.06
Gd Tb	5.07 0.86	5.15 0.7	4.37 0.55	5.83 0.8	4.41 0.63	4.78 0.65	4.26 0.59	5.6 0.89	6.67 0.92	5.22 0.82	5.43 0.86	5.53 0.88	4.14 0.58	5.71 0.97	5.26 0.8	5.33 0.73
Dy	5.05	3.42	2.42	4.15	3.04	3.14	2.79	5.24	4.5	4.62	5.04	5.1	2.96	5.85	3.94	3.56
Ho	1.01	0.46	0.35	0.63	0.5	0.51	0.43	0.91	0.76	0.87	1.03	1.02	0.51	1.19	0.7	0.58
Er	2.55	0.89	8.0	1.38	1.07	1.03	1	2.32	1.72	2.32	2.65	2.61	1.3	3.22	1.59	1.26
Tm	0.37	0.11	0.08	0.18	0.15	0.14	0.14	0.34	0.23	0.35	0.39	0.4	0.18	0.48	0.21	0.16
Yb	2.14 0.33	0.57 0.07	0.46 0.06	0.96 0.13	0.86 0.12	0.78 0.11	0.84 0.12	1.99 0.31	1.42 0.2	2.25 0.32	2.29 0.35	2.46 0.36	1.09 0.16	2.8 0.39	1.26 0.2	0.89 0.13
Lu	0.33	0.07	0.00	0.13	0.12	0.11	U. 12	0.51	0.2	0.32	0.33	0.30	0.10	0.59	0.2	0.13

The major elements are notably decoupled;  $TiO_2$ ,  $Al_2O_3$ , MgO, and  $FeO_{total}$  are well correlated with  $SiO_2$  but CaO,  $Na_2O$ ,  $K_2O$  and  $P_2O_5$  are not. In contrast to differentiated calc-alkaline granitoids, in these rocks the saturation in alumina decreases with increasing silica so

that the less silicic samples are notably more aluminous than the most silicic ones (Fig. 3). Noticeably, these lack such geochemical features as low K/Rb, low Zr/Hf, etc., that characterize highly differentiated granite rocks (*e.g.* Taylor *et al.*, 1956; Bea *et al.*, 2006a).

TABLE 1. (Cont.)

	R17	R18	R19	R20	R21	R22	R23	R24	R25	R26	R27	R28	R29	R30	R31	R32
SiO <sub>2</sub>	66.8	66.29	66.24	73.41	70.19	67.05	67.5	66.84	58.79	69.71	70.33	68.54	70.67	68.02	67.02	69.11
TiO <sub>2</sub>	0.55	0.61	0.79	0.29	0.42	0.52	0.54	0.5	1.05	0.45	0.36	0.59	0.54	0.68	0.64	0.49
$Al_2O_3$	16.28	15.79	14.83	13.72	15.02	15.62	15.7	15.56	18.07	15.29		15.235	14.44	15.34	16.55	15.69
FeO <sub>tot.</sub>	3.12	3.73	4.71	1.45	2.86	2.93	2.99	3.19	6.24	3.14	2.16	3.50	3.45	3.73	4.29	2.56
MgO <sup>tot.</sup>	1.47	1.82	2.49	0.45	1.06	1.53	1.49	1.51	3.33	1.14	0.69	1.47	0.92	1.44	1.63	1.45
MnO	0.04	0.06	0.08	0.03	0.05	0.04	0.04	0.04	0.09	0.05	0.03	0.05	0.04	0.05	0.057	0.04
CaO	1.22	1.48	1.75	0.74	0.89	0.98	0.91	1.48	1.45	0.93	0.79	1.07	1.08	1.28	1.31	0.73
$Na_2O$	3.01	2.75	2.78	2.92	2.85	2.82	2.96	2.75	2.82	2.75	3.99	2.66	3.35	2.17	2.26	4.06
K <sub>2</sub> O	4.53	4.18	3.43	5.25	4.54	5.17	4.68	4.55	3.17	4.43	4.70	4.26	4.08	4.39	4.11	3.5
P <sub>2</sub> O <sub>5</sub>	0.22	0.22	0.25	0.17	0.25	0.21	0.22	0.22	0.21	0.23	0.02	0.15	0.19	0.25	0.19	0.19
LOI	1.98	2.53	2.09	1.33	1.54	2.67	2.59	2.91	3.95	1.85	0.89	1.86	0.59	1.66	1.38	1.85
Total	99.22	99.46	99.44	99.76	99.67	99.55	99.62	99.55	99.17	99.97	99.49	99.39	99.35	99.01	99.43	99.67
Li	50	76	187	111	93	48	57	54	53	108	100	138	263	122	61	45
Rb	160	160	139	218	235	186	162	160	93	217	151	196	206	174	165	60
Cs	4.2	24	8.9	22.7	10.2	5.3	5.9	5.3	4.1	10.7	17.4	14.5	50.7	20.6	7.4	4.1
Be C-	2.5	2.3	2.5	5.1	1.9	2.4	2.6	2.7	4.2	1.8	1.5	2.6	2.3	2.9	2.7	3
Sr Ba	152 892	131 646	169 665	53 359	84 414	113 931	166 909	167 707	207 1063	92 424	78 421	116 570	125 753	129 757	134 696	32 614
Sc	8.5	11.1	17.4	3.8	7.8	8.2	8.4	7.4	20	7.5	4.5	10.7	8.8	9.4	11.2	3.8
V	54.6	70.1	115.9	16.6	46.3	51.2	52.8	48.6	129.3	48.7	29.7	67.2	53	63.3	70.5	47.7
<b>C</b> r	45.5	56	83.7	5.4	41.3	43.4	42.7	46.7	105.9	39.5	25.9	51.4	41.8	46.7	59.8	35.5
Ni	10.6	21.5	34	2.7	14	15.7	15.6	15	35.2	20.1	5.4	11.5	16.2	22.1	11.5	15.3
Cu	10.2	12.9	23.4	6.1	13	10.1	14.7	14.6	27.7	22.8	21.9	10.6	16.6	15.4	8.6	10.1
Zn	54.4	80.3	94.8	39.3	70.6	46.8	46.6	52.7	119.2	65.5	49.9	73.1	78.1	74.7	82.3	26.8
Ga	20.9	21.5	21.9	18.7	19	19.5	20.9	19	25	19.8	17.6	21.2	18.4	22	22.8	19.3
Υ	28.9	38.3	18.3	18.4	13.2	34	33.6	32.5	36.2	13	9.6	14.9	17.8	21.6	13.8	14.8
Nb	10.5	11.3	14.3	9.5	11.2	10	10.3	9.2	14.3	10.9	8.5	11.5	10	11.3	12.2	11.6
Ta	1	1.1	1.2	1.5	1.3	0.9	1	0.9	1.1	1.2	0.9	1.2	1	1.2	0.9	1.1
Zr	189	193	203	136	131	191	165	179	290	138	134	191	182	217	199	172
Hf	6.3	6.2	5.7	4.3	4.2	6	5.2	5.5	8.5	4.3	4.2	4.9	5	5	4.3	5.3
Мо	0.2	0.4	1	0.2	0.6	0.7	0.7	0.6	0.9	0.5	0.4	0.8	0.2	0.6	0.8	0.2
Sn	5.7	8.8	5.4	14.3	4.5	5.5	5	4.9	2	5.3	2.4	6.4	3.2	4.6	4.1	2.4
TI Pb	0.88 25.3	0.91 20.4	0.79	1.31	1.42	1.06	0.97	0.94 28.1	0.52	1.28	0.87	1.15	1.16	0.97	1.03	0.72 16.5
U	3.26	3.73	18.3 2.4	20.6 2.56	25.5 6.11	26.4 3.72	29.4 2.86	3.6	22.9 2.15	24.9 7.89	28.4 3.14	25 3.91	48.3 2.73	18.9 3.12	29.1 3.25	2.82
Th	12.76	12.38	10.95	10.59	11.73	13.57	14.2	11.77	16.73	11.18	8.27	16.96	12.07	12.5	14.2	5.78
La	35.9	33.2	34.5	20	26.7	25.7	34.7	27.7	55.8	26.5	20.4	37.6	30.4	35.2	37.2	16
Ce	74.3	67.8	71.1	43.8	56.7	54.7	74.4	58	110.6	55.7	45.1	75.8	63.6	74.3	77.8	39.8
Pr	9.01	8.37	8.74	5.27	7.09	6.51	8.82	6.93	13.76	6.91	5.46	9.06	7.73	8.99	9.06	4.04
Nd	33.9	32.8	33.5	19.5	27.5	25	31.8	28.5	50.8	26.7	20.9	33.5	29.7	35.4	34.6	15.3
Sm	7.22	7.12	7.03	4.76	5.74	5.76	6.82	6.29	10.22	5.53	4.78	6.74	6.11	7.07	7.07	3.19
Eu	1.39	1.17	1.25	0.51	0.78	1.15	1.31	1.2	2.1	0.84	0.75	1.04	1.03	1.16	1.13	0.62
Gd	6.57	6.78	6.1	4	4.56	5.68	6.15	5.79	9	4.42	3.32	5.23	4.93	6.02	5.54	2.76
Tb	1.08	1.08	0.83	0.64	0.65	0.91	1.03	0.91	1.34	0.61	0.42	0.73	0.73	0.83	0.76	0.42
Dy	5.78	6.43	4.15	3.66	2.99	5.43	5.86	5.29	7.14	2.78	2.06	3.4	3.7	4.24	3.58	2.62
Ho	1.04	1.34	0.72	0.66	0.46	1.14	1.14	1.07	1.31	0.47	0.35	0.55	0.64	0.76	0.55	0.55
Er	2.45	3.5	1.64	1.62	1.06	2.96	3.12	2.95	3.28	1.1	0.88	1.26	1.49	1.76	1.18	1.5
Tm	0.32	0.5	0.21	0.23	0.15	0.46	0.45	0.43	0.48	0.15	0.12	0.17	0.21	0.25	0.16	0.24
Yb	1.75	2.98	1.23	1.39	0.94	2.87	2.61	2.52	2.95	0.87	0.73	1.03	1.15	1.52	0.87	1.5
Lu	0.23	0.42	0.17	0.21	0.13	0.4	0.41	0.37	0.46	0.13	0.11	0.15	0.17	0.21	0.12	0.22

Chondrite-normalized REE patterns are parallel for LREE and MREE but diverge considerably for the heaviest REE (Fig. 5). La $_{\rm N}$  is typically between 100 and 200, decreasing to Sm $_{\rm N}$  between 30 and 60, with a small negative Eu anomaly between Eu/Eu\* $\approx$ 0.53-0.65 and Lu $_{\rm N}$  between 2 and 20. La $_{\rm N}$ /Lu $_{\rm N}$  is between 7 and 60.

NMORB-normalized spidergrams (Fig. 6) show a marked enrichment with increasing incompatibility, especially for the mica-hosted elements Rb and Cs, with notable troughs in Nb, Ti and Sr, and peaks in K and Pb. They however, lack the enrichment in Sr and moderate depletion in Zr characteristic of true arc-magmas.

The Sr and Nd isotope compositions of the Ollo de Sapo (Table 2) are clearly crustal: <sup>87</sup>Sr/<sup>86</sup>Sr<sub>485Ma</sub> is within the 0.7094 to 0.7113 interval (at 95% confidence) and clusters at 0.7103; the εNd<sub>485Ma</sub> is within the -4.76 to -4.23 interval (at 95% confidence) and clusters around -4.5 (Fig. 7A). It is worth mentioning that in a <sup>87</sup>Rb/<sup>86</sup>Sr vs. <sup>87</sup>Sr/<sup>86</sup>Sr plot most points scatter along the 485Ma reference line (Fig. 7C) so that, excluding the sample with the highest <sup>87</sup>Rb/<sup>86</sup>Sr, the remaining 27 samples fit an errorchron at 493±27Ma which nearly matches the average U-Pb zircon age (see next section). The goodness-of-fit of the errorchron despite the large sampled area and variable metamorphic grade indicates that the Ollo de Sapo rocks were not heavily disturbed during the Variscan metamorphism.

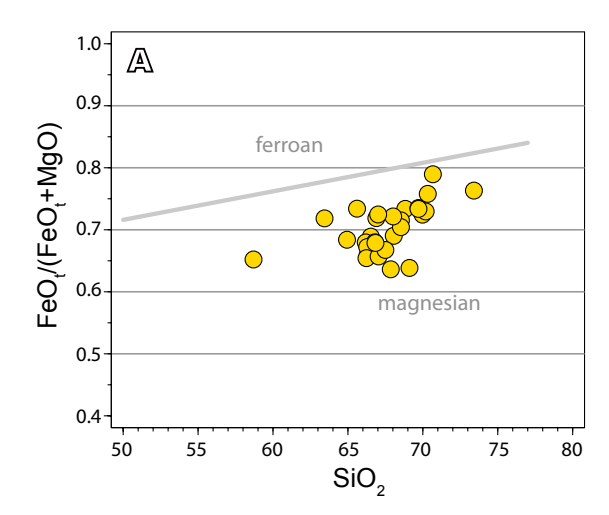
The Nd  $T_{\rm DM}$  model age distribution is asymmetric; it peaks a 1.5Ga and shows a large tail towards higher values with a minor peak at 1.8Ga (Fig. 7B). The 1.5Ga value is very common in Iberia and northern Africa (*e.g.* Bea *et al.*, 2010) but finds no correspondence with the U-Pb zircon ages. Bea *et al.* (2011) interpreted this value as a "mixed" Nd model age that is characteristic of most Pan-African granitoids generated throughout the Saharan metacraton.

#### **ZIRCON DATA**

# U-Pb ages

As mentioned in previous sections, the Ollo de Sapo zircons are distinctive because ~70-80%, in some cases up to 100%, contain pre-magmatic zircons (Bea *et al.*, 2006b; Montero *et al.*, 2007; Montero *et al.*, 2009; Talavera *et al.*, 2013). The data obtained by these authors in the zircon rims indicate that the magmatism of the Ollo de Sapo Formation started at about 495Ma, reached its maximum at 485Ma, and ended at about 470Ma (Fig. 8). The pre-magmatic cores show a wide range of inherited dates from Ediacaran to Mesoarchean but most of them are Neoproterozoic, mainly Ediacaran, with ages between 590Ma and 620Ma.

The three new samples studied here fit this pattern. The orthogneiss R19 (Fig. 8) yielded an age of 483±3Ma (2s) in the rims (22 data), which we consider the crystallization age. Most cores cluster around 600Ma but there are minor populations at *ca*. 680Ma, 890Ma, 970Ma and 2525Ma. The coarse-grained metavolcanic rock R32 (Fig. 8) yielded a rim age of 482±2Ma (51 data). The Ediacaran cores define a broad peak which likely indicates provenance from several sources with slightly different ages. A few cores yielded older-than-Ediacaran ages, up to Mesoarchean. Sample R31, a metavolcanic rock from the top of the sequence has the youngest rims with an age



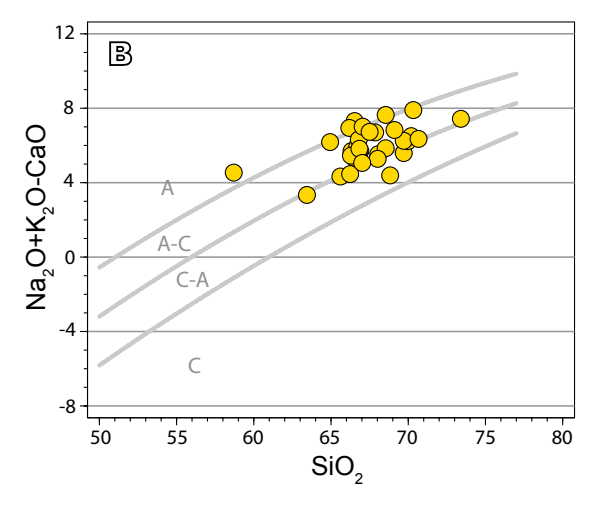


**FIGURE 2.** Frost *et al.* (2001) plots for the classification of granite rocks. The Ollo de Sapo rocks are magnesian (A) and alkaline-calcic to calc-alkaline (B).

of 478±4Ma (Fig. 8). The Ediacaran cores peak at 615Ma, but the peak asymmetry suggests the contribution of another population at 590Ma-600Ma.

# Oxygen isotopes

Zircons from the three low-grade samples studied for oxygen isotopes show the same picture: the Cambrian-Ordovician rims are more enriched in the heaviest oxygen than the Ediacaran and older cores (Fig. 9).

The rims yielded unimodal, nearly gaussian distributions that cluster around  $\partial^{18}O=10$ , values which are typical of S-type magmas formed from melting of altered crust. The cores, however, are considerably impoverished in the heaviest oxygen, with  $\partial^{18}O$  clustering around 6.5. The oxygen isotope distribution in the cores is unimodal for samples R31 and R32 but shows a minor  $\partial^{18}O$  mode around 8.5 in the orthogneiss R19. The 6.5

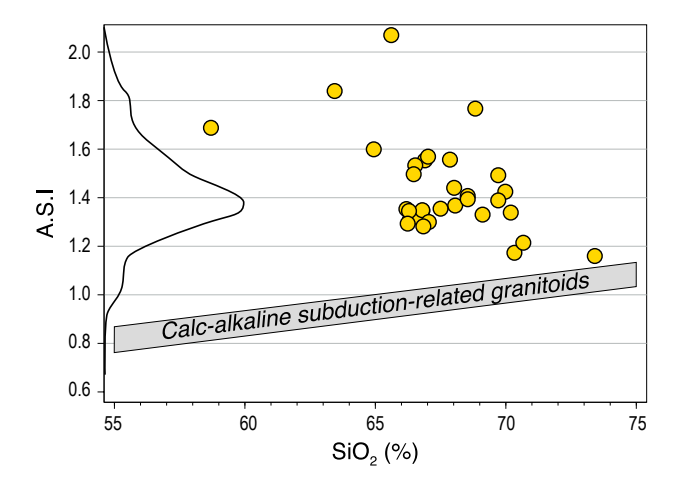


**FIGURE 3.** Aluminium Saturation Index (ASI=mol. Al $_2$ O $_3$ /CaO + Na $_2$ O + K $_2$ O) vs. SiO $_2$ . The area corresponding to calc-alkaline subduction-related granites was drawn using more than 1000 analyses from different plutons of the Urals and the circum-Pacific batholiths of America. The curve along the left Y axis is the density distribution of the analyzed samples. Whereas in calc-alkaline granites the A.S.I. increases with silica, in the Ollo the Sapo gneisses it decreases. This suggests that the major element chemistry of these rocks is controlled by restite unmixing. See text for discussion.

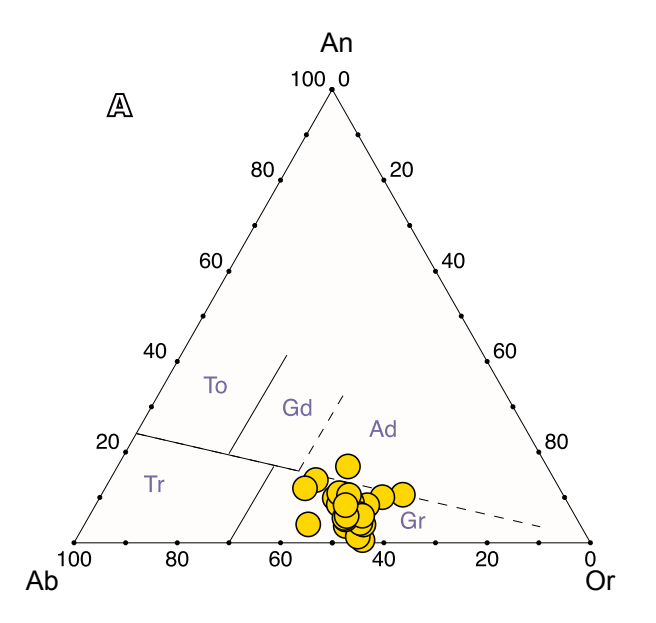
mode is about one per mil higher than typical mantle values but of the same order as subduction-related granites (Valley, 2003); they indicate that the cores of the Ollo de Sapo zircons crystallized from magmas that were either derived from primitive sources slightly altered with low temperature fluids or were contaminated with metasediments.

#### Hafnium isotopes

The Hf isotope compositions of rims and cores overlap, but the former are considerably more homogeneous (Fig. 10). In the rims, the  $\varepsilon Hf_{485Ma}$  spans from -6.4 to 2.6 with a mean of -2.1. The distribution in the two metavolcanic rocks is sharply unimodal (Fig. 11) albeit peaking at different values (-0.4 the fine-grained, and -3.4 the coarse-grained metavolcanites). The metagranite R19, however, is bimodal, with a lower mode at  $\varepsilon Hf_{485Ma}$ =-0.2 and a higher mode at  $\varepsilon Hf_{485Ma}$ =1.6. On the other hand, the distribution of  $\varepsilon Hf_{600Ma}$  in the Ediacaran cores is polymodal, notably more irregular than in the rims.

The Hf model ages (calculated assuming a depleted mantle that changed from chondritic at  $\varepsilon Hf_{4.56Ga}=0$  to  $\varepsilon Hf_{0Ga}=+16$ , and a source with  $^{177}Lu/^{176}Hf=0.007$ , see Bea *et al.*, *Submitted*) range between 1.1 and 1.5Ga with a mean of 1.3Ga but, again, the average values for each sample are markedly different, mimicking somehow the distribution of  $\varepsilon Hf_{485Ma}$ .

The cores are more heterogeneous than rims. Twentynine Pan-African cores yielded  $\epsilon Hf_{485Ma}$  from -9.4 to 9.8 with a mean of -0.02, and Hf model ages from 0.8 to 2.4Ga with mean at 1.34Ga. Remarkably, the average of rims and cores are nearly identical despite the largest variation of the latter. Lastly, eleven older-than-Panafrican cores yielded  $\epsilon Hf_T$  from -22 to 4.6 and the Hf  $T_{DM}$  from 1.7 to 3.2Ga so indicating the contribution of Paleo-Proterozoic to Archean components to the source.



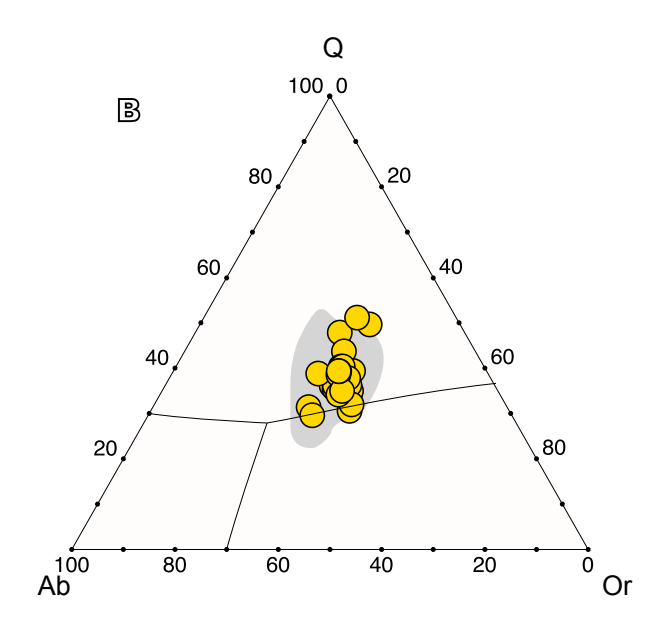


**FIGURE 4.** Proportions of normative (CIPW) components of Ollo de Sapo gneisses A) Ab-Or-An plot; fields are those delimited by O'Connor (1965). Note how all the gneisses plot in the field of granites s.s. B) Ab-Or-Q plot; phase boundaries are those determined by Luth *et al.* (1964) at  $P_{H2O}$ =5bar. The gray area corresponds to corundum-normative granites as calculated by the same authors. The Ollo de Sapo gneisses plot almost exactly in this gray area.

#### DISCUSSION

As mentioned in the Introduction, some authors have proposed a supra-subduction setting for the Ollo de Sapo and compared these rocks, either implicitly or explicitly, with I-type calc-alkaline subduction-related granite-rhyolite series. This hypothesis is based solely on the general enrichment in the most incompatible trace elements and depletion in Nb and Ti. It, however, is inconsistent with major element and Sr and Nd isotopes.

The lack of correlation between CaO, Na<sub>2</sub>O, K<sub>2</sub>O and P<sub>2</sub>O<sub>5</sub> with SiO<sub>2</sub> rules out that the Ollo de Sapo rocks might represent variably differentiated members of magma batches with a similar initial composition. Of particular relevance are the elevated peraluminosity of the less silicic samples and the negative correlation between ASI and SiO<sub>2</sub>. These features, which are never seen in arc-related calc-alkaline granite-rhyolite series (Fig. 3), suggest different degrees of restite unmixing in anatectic magmas derived from peraluminous sources. Moreover, Sr and Nd isotopes reveal that the magmatic sources contained no detectable juvenile components and so must have resided in the crust long before the Cambrian-Ordovician melting event.

It might be argued that the original chemical and isotopic features of the Ollo de Sapo rocks were profoundly disturbed by the Variscan metamorphism, or that the spatial heterogeneity of the magmatic sources masked the interelement correlations characteristic of felsic arc-magmas. However, none of these ideas find support from Sr isotopes as shown by the excellent match between the twenty-seven samples Rb-Sr errorchron age (493±27Ma; Fig. 7) and the SHRIMP zircon U-Pb ages (Fig. 8) mentioned before.

Geochemical evidence, therefore, is inconsistent with a supra-subduction setting but rather points to an intracontinental origin. The magmatic arc-like trace element features can be attributed to inheritance from the magma source which consisted of rocks with abundant Ediacaran zircons. The question is now to understand whether these sources consisted of Ediacaran igneous rocks with some older zircon components, or younger immature sediments derived from them, a question first raised by Montero *et al.* (2007).

The answer comes from the zircon oxygen isotope compositions. All rims without exception have an elevated  $\partial^{18}O$  of around 10. This implies a source with whole-rock  $\partial^{18}O$  close to 12 which is a typical "sedimentary" value absolutely uncharacteristic of fresh igneous rocks from magmatic arcs (Valley, 2003, and references therein). The oxygen isotope composition of the 600-615Ma cores, in contrast, is

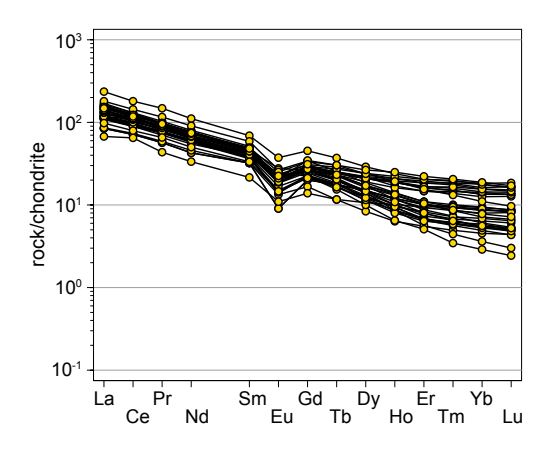


**FIGURE 5.** Chondrite-normalized REE patterns of the Ollo de Sapo gneisses. They are parallel for LREE and MREE but diverge considerably for the heaviest REE.

around  $\partial^{18}O\approx6$ , thus compatible with Ediacaran magmas being arc-derived. Accordingly, the contrasting oxygen isotope composition of Cambrian-Ordovician rims and Ediacaran cores indicates that the Ollo de Sapo magmatic sources likely consisted of detrital sediments mainly derived from Ediacaran igneous rock rather than the Ediacaran igneous rocks themselves. Considering zircon ages and composition (Talavera *et al.*, 2012) the most likely candidates are the graywackes of the Schist-Graywacke-Complex, the dominant Central Iberian meta-sedimentary formation (*e.g.* Rodríguez Alonso *et al.*, 2004, and references therein).

A sedimentary source explains the large variability of U-Pb ages and Hf isotopes in the Ediacaran cores (Figs. 8 and 10). If we accept that the Ollo de Sapo magmas were swiftly produced and emplaced high in the crust, as suggested by the abnormally high zircon inheritance (Bea

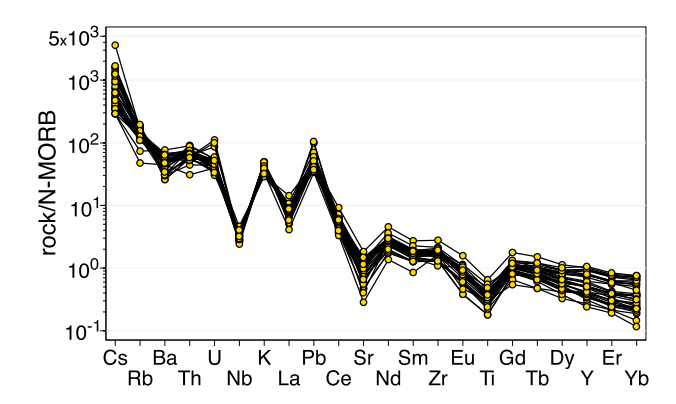


**FIGURE 6.** N-MORB-normalized spidergrams. Note the marked enrichment with increasing incompatibility, the troughs in Nb, Ti and Sr, and the peaks in K and Pb. These patterns lack the enrichment in Sr and moderate depletion in Zr characteristic of true arc-magmas.

TABLE 2. Isotope composition of the Ollo de Sapo gneisses. See text

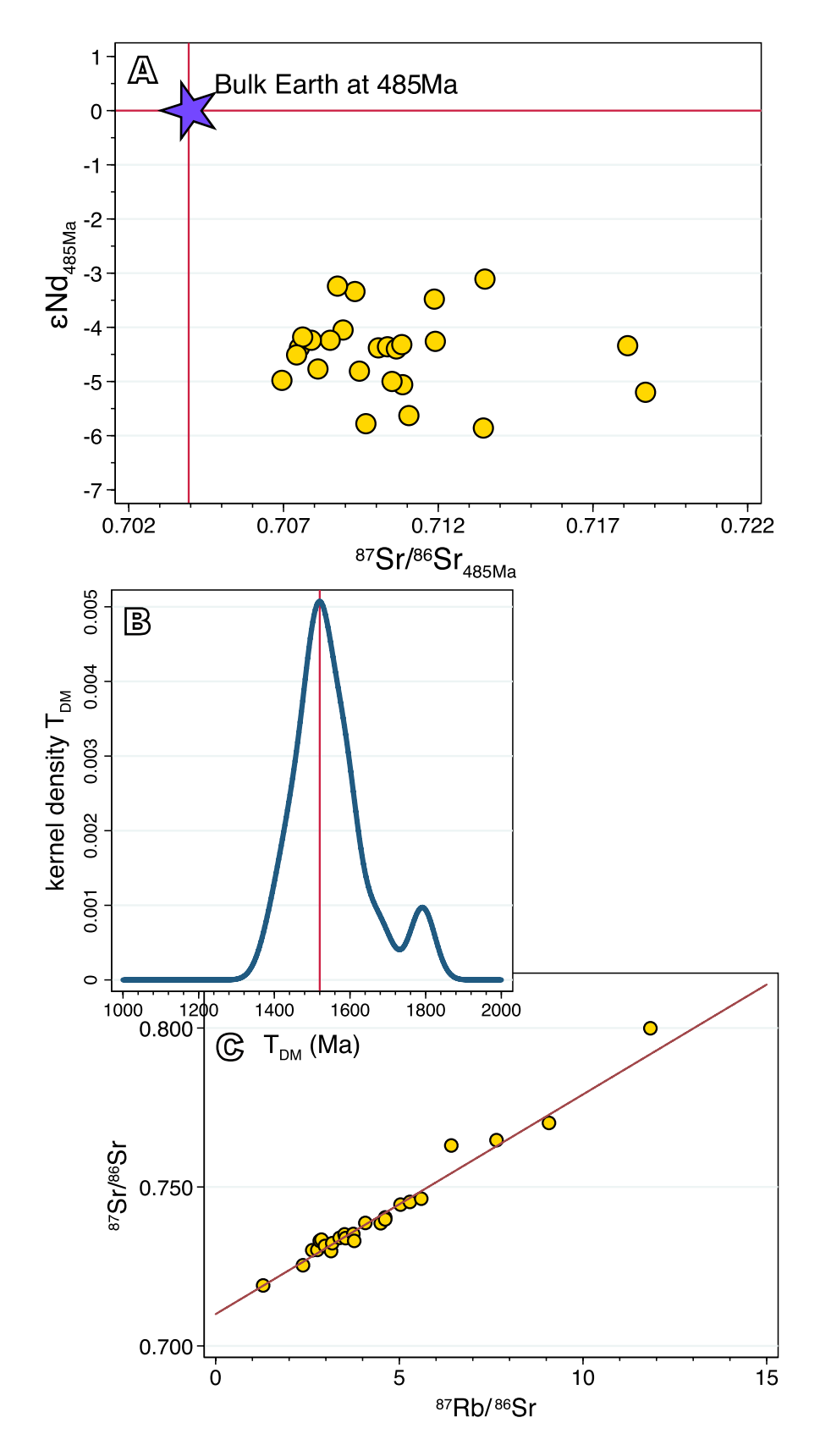
id	<sup>87</sup> Rb/ <sup>86</sup> Sr	<sup>87</sup> Sr/ <sup>86</sup> Sr	<sup>87</sup> Sr/ <sup>86</sup> Sr	εSr	<sup>147</sup> Sm/ <sup>144</sup> Nd	<sup>143</sup> Nd/ <sup>144</sup> Nd	<sup>143</sup> Nd/ <sup>144</sup> Nd	$\epsilon \text{Nd}$	TDM (Ma)
				(485Ma)	(485Ma)		(485Ma)	(485Ma)	
R01	3.156	0.732715	0.710905	99.1	0.130	0.512219	0.511805	-4.07	1499
R05	6.117	0.751473	0.709202	74.9	0.128	0.512213	0.511806	-4.05	1469
R06	5.181	0.745464	0.709656	81.4	0.127	0.512206	0.511803	-4.11	1460
R07	6.935	0.757267	0.709341	76.9	0.125	0.512176	0.511778	-4.59	1484
R09	3.142	0.729827	0.708114	59.5	0.127	0.512172	0.511769	-4.77	1521
R10	6.115	0.754789	0.712528	122.2	0.126	0.512195	0.511796	-4.25	1459
R11	2.630	0.730082	0.711907	113.3	0.130	0.512208	0.511794	-4.29	1518
R12	2.976	0.731418	0.710851	98.3	0.131	0.512170	0.511754	-5.06	1597
R13	8.700	0.770138	0.710013	86.4	0.134	0.512208	0.511783	-4.50	1583
R14	3.175	0.732301	0.710362	91.4	0.130	0.512203	0.511790	-4.36	1519
R15	3.748	0.735207	0.709309	76.4	0.131	0.512258	0.511842	-3.34	1435
R16	5.442	0.746303	0.708698	67.8	0.128	0.512206	0.511800	-4.17	1478
R17	3.543	0.733897	0.709414	77.9	0.129	0.512202	0.511793	-4.30	1499
R18	3.536	0.733889	0.709453	78.5	0.131	0.512183	0.511766	-4.83	1580
R19	2.377	0.725354	0.708925	71.0	0.127	0.512209	0.511806	-4.05	1456
R20	11.835	0.799910	0.718123	201.7	0.147	0.512258	0.511790	-4.35	1787
R21	7.646	0.764712	0.711875	112.9	0.135	0.512264	0.511836	-3.46	1492
R22	5.033	0.744442	0.709663	81.5	0.139	0.512159	0.511717	-5.79	1796
R23	2.869	0.733046	0.713217	131.9	0.130	0.512126	0.511715	-5.83	1649
R24	2.768	0.730184	0.711052	101.2	0.133	0.512148	0.511724	-5.65	1688
R25	1.293	0.719005	0.710067	87.2	0.122	0.512177	0.511791	-4.34	1425
R26	5.288	0.745292	0.708745	68.4	0.135	0.512276	0.511848	-3.22	1470
R27	6.758	0.763038	0.716337	176.3	0.123	0.512138	0.511746	-5.21	1517
R28	5.038	0.742772	0.707953	57.2	0.131	0.512124	0.511708	-5.96	1681
R29	4.494	0.738573	0.707515	50.9	0.129	0.512199	0.511789	-4.38	1511
R30	3.610	0.733021	0.708076	58.9	0.131	0.512174	0.511759	-4.97	1585
R31	3.572	0.734102	0.709418	78.0	0.124	0.512198	0.511806	-4.05	1420
R32	5.506	0.747328	0.709277	76.0	0.126	0.512204	0.511804	-4.09	1450

et al., 2007), we must also accept that the so produced magmas could not have mixed over large volumes. Had the source been an igneous rock, the Hf isotope composition of their zircons would have been nearly uniform. If, on the other hand, the source consisted of sediments in which zircons were randomly accumulated as detrital particles coming from isotopically different Ediacaran rocks, the magmas generated from them would have had isotopically heterogeneous pre-magmatic zircons. However, as a result of homogenization of the melt phase, they would have crystallized nearly isotopically homogenous rims with a Hf composition close to the core average. This can explain the distribution of  $\varepsilon Hf_T$  in rims and cores of zircons from the Ollo de Sapo rocks depicted in Figure 11.

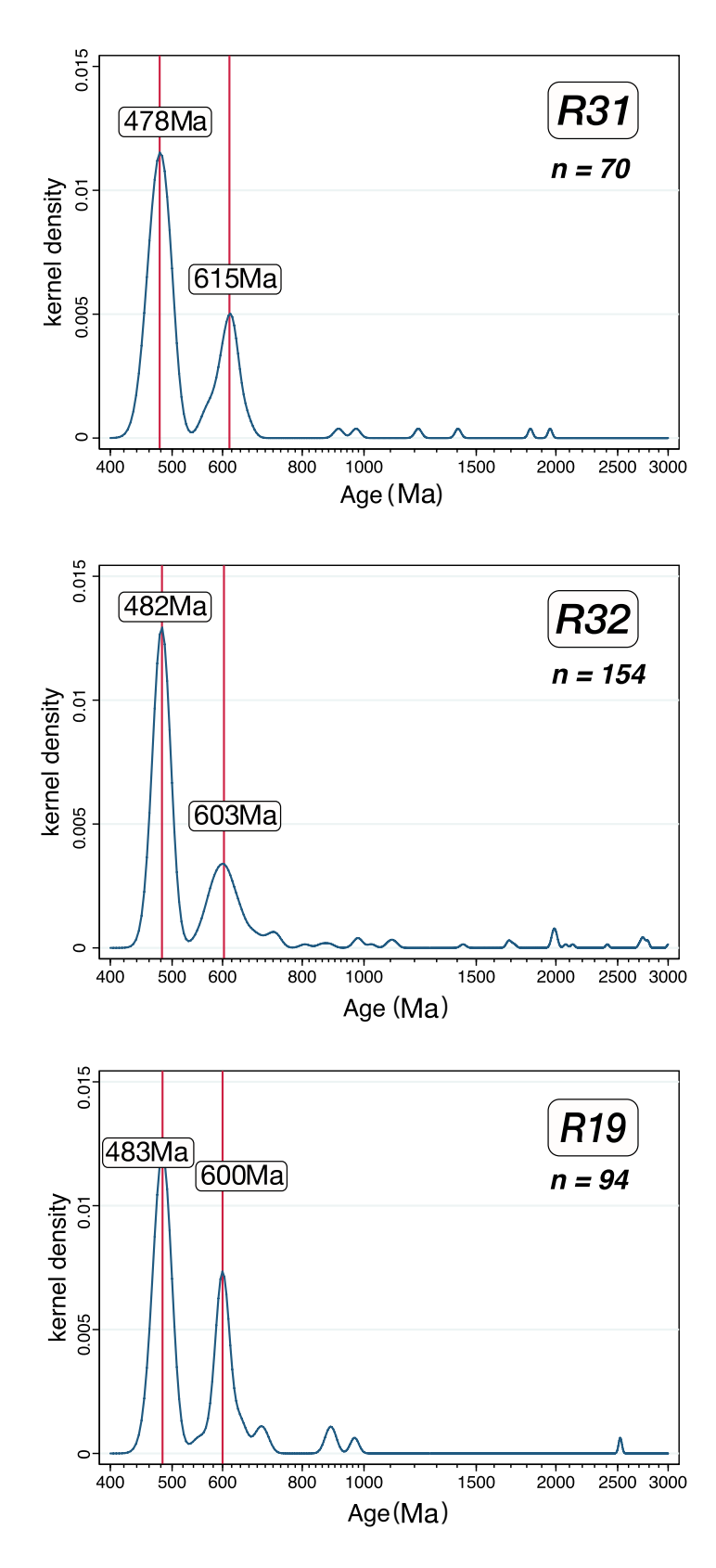
Lastly, a sedimentary source may also explain why the Hf  $T_{DM}$  of the zircons (1.3Ga) is significantly younger than the whole-rock Nd  $T_{DM}$  (1.5Ga). This effect suggest that the source, in addition to detrital materials coming from Ediacaran igneous rocks, also contained a small fraction of older materials with higher REE/Zr the remnants of which are the Mesoproterozoic to Archean zircon cores of the Ollo de

Sapo. Nevertheless, this suggestion must be considered with caution because calculating Hf  $T_{DM}$  model ages of zircons requires an assumption regarding average crust composition, and this introduces a difficult-to-evaluate uncertainty factor (see Vervoort and Kemp, 2016, and references therein). In the present case we tuned the calculations for the average composition of the pre-Variscan Iberian crust (Lu/Hf=0.045; submitted) which is remarkably uniform, but even using an average crust composition (Lu/Hf=0.09; Rudnick and Fountain, 1995) the Hf  $T_{DM}$  yields 1.35Ga, which is still younger than the Nd  $T_{DM}$ .

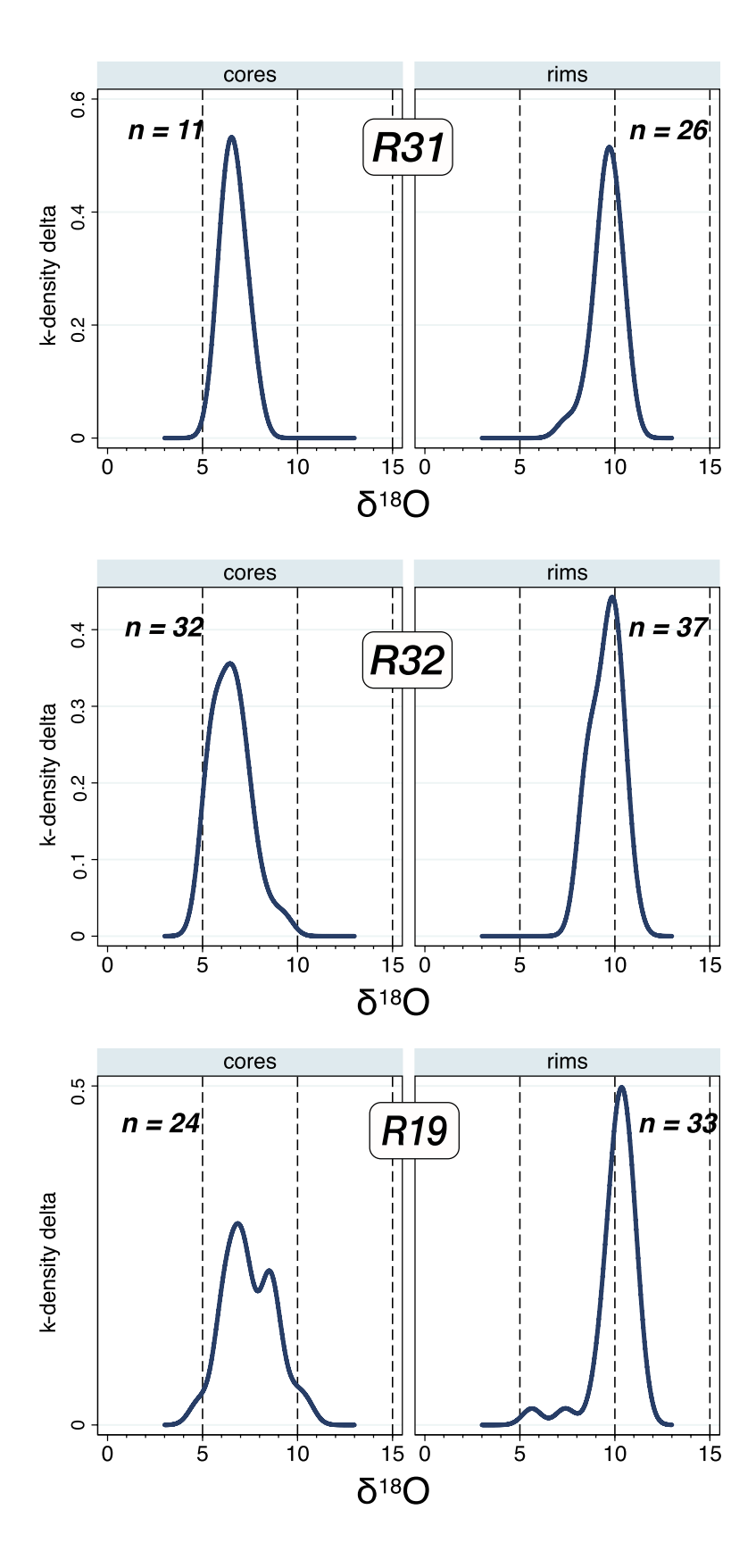
Accordingly, we infer that the Ollo de Sapo magmas were produced by melting of (meta) sedimentary sources that mostly, but not solely, derived from 600-615Ma polygenic igneous rocks. Currently, no examples of such materials are known in Central Iberia. The only Ediacaran rocks precisely dated are the 580±3Ma Aljucén gabbrodiorites (Talavera *et al.*, 2008) and, close to the Cambrian boundary, the 543±6 Almohalla granodiorites (Bea *et al.*, 2003) so that the main component of the Ollo de Sapo magmatic sources remains hidden to direct observation. Nonetheless, considering the



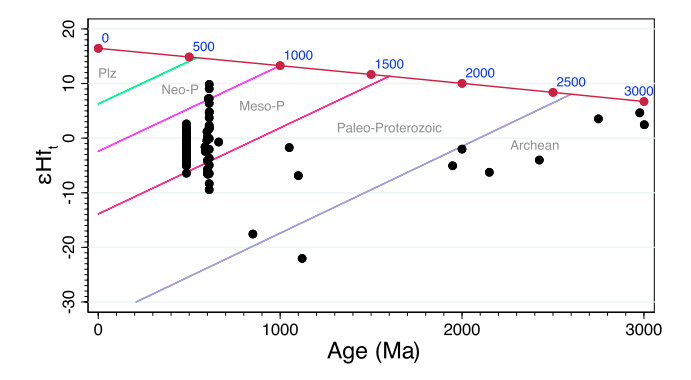
**FIGURE 7.** A) <sup>87</sup>Sr/<sup>86</sup>Sr<sub>485Ma</sub> vs. £Nd<sub>485Ma</sub> for the Ollo de Sapo gneisses. No juvenile components are detected. B) Frequency plot of the Nd T<sub>DM</sub> model age (DePaolo, 1981). The distribution peak at 1.5Ga, is asymmetric toward the highest values and has a minor mode at 1.8Ga. C) Rb-Sr errorchron built with 27 Ollo de Sapo gneisses. The age is 493±27Ma, *i.e.* within the error range of the zircon U-Pb crystallization age. See text for discussion.



**FIGURE 8.** Frequency diagram of the U-Pb ages in the three studied samples (raw data in ELECTRONIC APPENDIX I (available at www.geologica-acta.com), Tables I, II, and III). Ages younger than 500Ma correspond to zircon rims; ages older than 500Ma are always pre-magmatic cores. The crystallization ages, 483±3Ma for the metagranite, 482±2Ma for the lower metavolcanite and 478±4Ma for the upper metavolcanites are close to the age of maximum magma production, *ca.* 485Ma (Montero *et al.*, 2009, and references therein). Note how the most abundant pre-magmatic cores are Ediacaran although minor Cryogenian and Tonian populations can also be recognized.

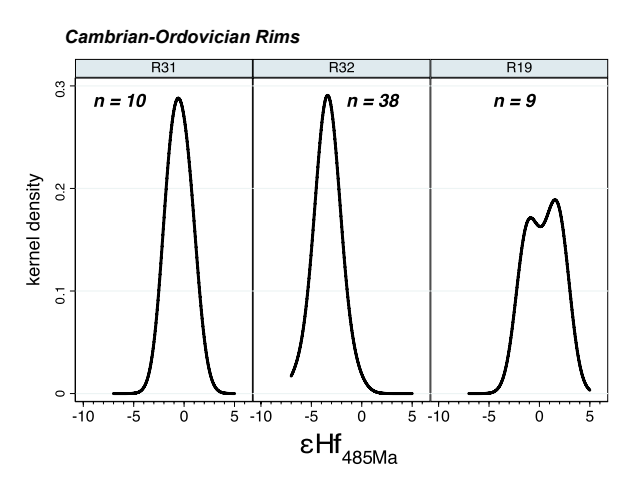


**FIGURE 9.**  $\partial^{18}$ O distribution in zircon rims and cores of the studied samples (raw data in ELECTRONIC APPENDIX I, Table IV). The rims are enriched in  $^{18}$ O thus indicating derivation from metasediments. The composition of the cores, however, is consistent with magmas rich in juvenile components and little participation of sedimentary materials. See text for discussion.



**FIGURE 10.**  $\epsilon Hf_{485Ma}$  vs. time plot (raw data in ELECTRONIC APPENDIX I, Table V). The much higher variability of the Ediacan cores (see Fig. 11) suggests these came from isotopically heterogeneous sources with a similar age.

chemical and isotopic composition of the Ollo de Sapo rocks and the ages of the inherited zircons, we propose that this component would have not be very different to the



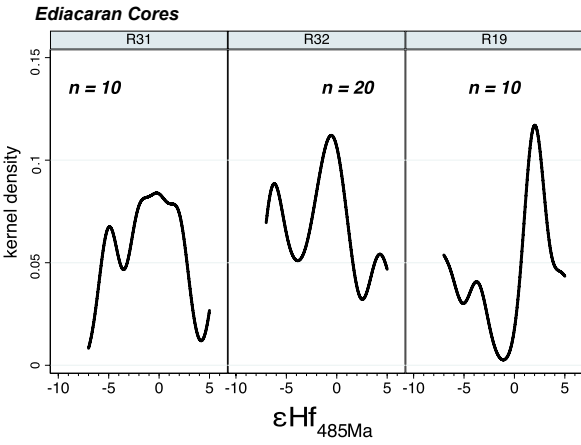


**FIGURE 11.** Kernel density distributions of  $\epsilon Hf_T$  in Cambro-Ordovician rims and Ediacaran cores of zircons from the Ollo de Sapo Formation. The difference between rims and cores suggests the magmatic source was composed of metasedimentary rocks derived from Ediacan granitoids.

Pan-African granitoids of North-East Africa from which Central Iberia detached during the Cambrian-Ordovician (see Bea *et al.*, 2010; 2011, and references therein).

#### SUMMARY AND CONCLUSIONS

The Ollo de Sapo gneisses are Cambrian-Ordovician S-type granitoids that contain an abnormally elevated proportion of zircons with premagmatic cores, most of which are Ediacaran.

The gneiss major element compositions correspond to peraluminous felsic melts in which the saturation in alumina decreases with increasing silica. This is the opposite of what occurs in fractionated calc-alkaline series and indicates that the chemical variability of the Ollo de Sapo gneisses mainly resulted from variable unmixing of peraluminous restites from felsic near-haplogranitic melts.

The gneiss Sr and Nd isotope compositions ( ${}^{87}\text{Sr}/{}^{86}\text{Sr}_{485\text{Ma}}$ =0.7104±0.00008,  $\epsilon \text{Nd}_{485\text{Ma}}$ =-4.50±0.26) are decidedly crustal, indicating their sources contained little, if any juvenile material.

The trace element compositions bear some similarities to high-K calc-alkaline rocks from subduction settings such as the enrichment in the most incompatible elements, depletion in Nb and Ti, and peaks in K and Pb but lack the enrichment in Sr and moderate depletion in Zr characteristic of true arc-magmas.

The Ollo de Sapo zircons are markedly bimodal with respect to oxygen isotopes. Whereas the Cambrian-Ordovician rims yielded unimodal distributions that cluster around  $\partial^{18}\text{O}=10$ , typical of S-type magmas formed from melting of altered crust, the Ediacaran cores cluster around  $\partial^{18}\text{O}=6.5$ , typical of arc-magmas. Rims and cores have the same average Hf isotope composition but the former are much more homogeneous.

The elevated  $\partial^{18}O$  of the Cambrian-Ordovician zircon rims reveals that the Ollo de Sapo gneisses are in fact S-type granites and rhyolites that resulted from anatexis of younger-than-600Ma immature sediments. These sediments mostly, but not solely, derived from different Ediacaran igneous rocks with a wide range of Hf isotope composition. Despite the lack of direct field evidence, zircon data suggest that the metasedimentary sources of the Ollo de Sapo were the graywackes that form part of the Schist-Graywacke Complex.

The abundance of inherited zircons indicates that melting and emplacement occurred with little fractionation and discharge of suspended solids. This indicates that the arc-like trace element features were inherited from the sedimentary sources formed from erosion of Ediacaran arc-like igneous rocks.

Our data preclude that the Ollo de Sapo rocks might have resulted from arc-related magmatism and lend support to the idea of generation in an extensional regime as proposed by Bea *et al.* (2007) and Díez Montes *et al.* (2010).

#### **ACKNOWLEDGMENTS**

This paper has been financed by the Spanish Grant CGL2013-40785-P, and the Andalusian Grant P12.RNM.2163. This is the IBERSIMS publication  $n^{\circ}$  39.

#### REFERENCES

- Bea, F., Montero, P., Zinger, T., 2003. The Nature and Origin of the Granite Source Layer of Central Iberia: Evidence from Trace Element, Sr and Nd Isotopes, and Zircon Age Patterns. Journal of Geology, 111, 579-595.
- Bea, F., Montero, P., Ortega, M., 2006a. A LA-ICPMS evaluation of Zr reservoirs in common crustal rocks: implications for Zr and Hf geochemistry, and zirconforming processes. Canadian Mineralogist, 44, 693-714.
- Bea, F., Montero, P., Talavera, C., Zinger, T., 2006b. A revised Ordovician age for the oldest magmatism of Central Iberia: U-Pb ion microprobe and LA-ICPMS dating of the Miranda do Douro orthogneiss. Geologica Acta, 4, 395-401.
- Bea, F., Montero, P., González Lodeiro, F., Talavera, C., 2007. Zircon inheritance reveals exceptionally fast crustal magma generation processes in Central Iberia during the Cambro-Ordovician. Journal of Petrology, 48, 2327-2339.
- Bea, F., Montero, P., Talavera, C., Abu Anbar, M., Scarrow, J.H., Molina Palma, J.F., Moreno, J.A., 2010. The palaeogeographic position of Central Iberia in Gondwana during the Ordovician: evidence from zircon chronology and Nd isotopes. Terra Nova, 22, 341-346.
- Bea, F., Montero, P., Abu Anbar, M., Molina, J.F., Scarrow, J., 2011. The Bir Safsaf Precambrian inlier of South West Egypt revisited. A model for ~ 1.5Ga TDM late Pan-African granite generation by crustal reworking. Lithos, 125, 897-914.
- Black, L.P., Kamo, S.L., Allen, C.M., Aleinikoff, J.A., Davis, D.W., Korsch, J.R., Foudolis, C., 2003. TEMORA 1: a new zircon standard for Phanerozoic U-Pb geochronology. Chemical Geology, 200, 155-170.
- Chu, N.C., Taylor, R.N., Chavagnac, V., Nesbitt, R.W., Boella, R.M., Milton, J.A., German, C.R., Bayon, G., Burton, K., 2002. Hf isotope ratio analysis using multi-collector inductively coupled plasma mass spectrometry: an evaluation of isobaric interference corrections. Journal of Analytical Atomic Spectrometry, 17, 1576-1574.

- Cumming, G.L., Richards, J.R., 1975. Ore lead isotope ratios in a continuously changing Earth. Earth and Planetary Science Letters, 28, 155-171.
- Del Greco, K., Johnston, S.T., Shaw, J., 2016. Tectonic setting of the North Gondwana margin during the Early Ordovician: A comparison of the Ollo de Sapo and Famatina magmatic events. Tectonophysics, 681, 73-84.
- DePaolo, D.J., 1981. Neodymium isotopes in the Colorado Front Range and implications for crust formation and mantle evolution in the Proterozoic. Nature, 291, 193-197.
- Díez Montes, A., Navidad, M., González Lodeiro, F., Martínez Catalán, J.R., 2004. El Ollo de Sapo. In: Vera, J.A., (ed.). Geología de España, Sociedad Geológica Española (SGE)-Instituto Geológico y Minero de España (IGME), Madrid, 69-72.
- Díez Montes, A., Martínez Catalán, J.R., Bellido Mulas, F., 2010. Role of the Ollo de Sapo massive felsic volcanism of NW Iberia in the Early Ordovician dynamics of northern Gondwana. Gondwana Research, 17(2-3), 363-376.
- Frost, B.R., Barnes, C.G., Collins, W.J., Arculus, R.J., Ellis, D.J., Frost, C.D., 2001. A geochemical classification for granitic rocks. Journal of Petrology, 42, 2033-2048.
- Gebauer, D., Martínez-García, E., Hepburn, J.C., 1993. Geodynamic significance, age and origin of the Ollo de Sapo Augengneiss (NW Iberian Massif, Spain). Proceedings from Geological Society of America, 1993 annual meeting, Abstracts with Programs 25-6, p.342.
- González Lodeiro, F., 1981. La estructura del anticlinorio del "Ollo de Sapo" en la región de Hiendelaencina (extremo oriental del Sistema Central Español). Cuadernos Geología Ibérica, 7, 535-545.
- Govindaraju, K., Potts, P.J., Webb, P.C., Watson, J.S., 1994.
  Report on Whin Sill Dolerite WS-E from England and Pitscurrie Micrograbbro PM-S from Scotland: assessment by one hundred and four international laboratories. Geostandards Newsletters, XVIII(2), 211-300.
- Gutiérrez Marco, J.C., Robardet, M., Rábano, I., Sarmiento, G.N., San José Lancha, M.A., Herranz, P., Pieren Pidal, A.P., 2002. Ordovician. In: Gibbons, W., Moreno, T. (eds.). The Geology of Spain. London, Geological Society, 31-49.
- Helbing, H., Tiepolo, M., 2005. Age determination of Ordovician magmatism in NE Sardinia and its bearing on Variscan basement evolution. Journal of the Geological Society, 162, 689-700.
- Ickert, R., Hiess, J., Williams, I., Holden, P., Ireland, T., Lanc, P., Schram, N., Foster, J., Clement, S., 2008. Determining high precision, in situ, oxygen isotope ratios with a SHRIMP II: Analyses of MPI-DING silicate-glass reference materials and zircon from contrasting granites. Chemical Geology, 257(1-2), 114-128.
- Iglesias Ponce de León, M., Ribeiro, A., 1981. Position stratigraphique de la formation Ollo de Sapo dans la région de Zamora (Espagne) - Miranda do Douro (Portugal). Comunicações do Servicio Geológico de Portugal, 67(2), 141-146.

- Laumonier, B., Autran, A., Barbey, P., Cheilletz, A., Baudin, T., Cocherie, A., Guerrot, C., 2004. On the non-existence of a Cadomian basement in southern France (Pyrenees, Montagne Noire): implications for the significance of the pre-Variscan (pre-Upper Ordovician) series. Bulletin de la Société Géologique de France, 175(6), 643-655.
- Luth, W.C., Jahns, R.H., Tuttle, O.F., 1964. The granite system at pressures of 4 to 10 kilobars. Journal of Geophysical Research, 69, 759-773.
- Montero, P., Bea, F., 1998. Accurate determination of <sup>87</sup>Rb/<sup>86</sup>Sr and <sup>147</sup>Sm/<sup>144</sup>Nd ratios by inductively-coupled-plasma mass spectrometry in isotope geoscience: an alternative to isotope dilution analysis. Analytica Chimica Acta, 358, 227-233.
- Montero, P., Bea, F., González-Lodeiro, F., Talavera, C., Whitehouse, M., 2007. Zircon crystallization age and protolith history of the metavolcanic rocks and metagranites of the Ollo de Sapo Domain in central Spain. Implications for the Neoproterozoic to Early-Paleozoic evolution of Iberia. Geological Magazine, 144(6), 963-976.
- Montero, P., Talavera, C., Bea, F., González-Lodeiro, F., Whitehouse, M.J., 2009. Zircon geochronology and the age of the Cambro-Ordovician rifting in Iberia. Journal of Geology, 117, 174-191.
- Navidad, M., Bea, F., 2004. El magmatismo prevarisco de la Zona Centroibérica. In: Vera, J.A. (ed.). Geología de España, Sociedad Geológica Española- Instituto Geológico y Minero de España (SGE-IGME), Madrid, 92-96.
- O'Connor, J.T., 1965. A classification for quartz-rich igneous rocks based on feldspar ratios. U.S. Geological Survey Professional Paper, 525B, B79-B84.
- Parga-Pondal, I., Matte, P., Capdevila, R., 1964. Introduction à la géologie de 'l'Ollo de Sapo', Formation porphyrode antesilurienne du nord ouest de l'Espagne. Notas y Comunicaciones del Instituto Geológico y Minero de España, 76, 119-153.
- Paton, C., Hellstrom, J., Paul, B., Woodhead, J., Hergt, J., 2011. Iolite: Freeware for the visualisation and processing of mass spectrometric data. Journal of Analytical Atomic Spectrometry, 26, 2508-2519.
- Peacock, M.A., 1931. Classification of igneous rock series. Journal of Geology, 39, 54-67.
- Rodríguez Alonso, M.D., Díez Bald, M.A., Perejón, A., Pieren,
  A.P., Liñán, E., López Díaz, F., Moreno, F., Gómez Vintanez,
  J.A., González Lodeiro, F., Martinez Poyatos, D., Vegas, R.,
  2004. 2.4.3.1. Estratigrafía: La secuencia litoestratigráfica
  del Neoproterozoico-Cámbrico Inferior. In: Vera, J.A. (ed.).
  Geología de España, Sociedad Geológica Española Instituto
  Geológico y Minero de España (SGE-IGME), Madrid, 78-81.
- Rudnick, R.L., Fountain, D.M., 1995. Nature and Composition of the Continental-Crust-a Lower Crustal Perspective. Reviews of Geophysics, 33, 267-309.

- Sola, A.R., Pereira, M.F., Williams, I.S., Ribeiro, M.L., Neiva, A.M.R., Montero, P., Bea, F., Zinger, T., 2008. New insights from U-Pb zircon dating of Early Ordovician magmatism on the northern Gondwana margin: The Urra Formation (SW Iberian Massif, Portugal). Tectonophysics, 461, 114-129.
- Talavera, C., Montero, M.P., Bea, F., 2008. Precise single-zircon Pb-Pb dating reveals that Aljucén (Mérida) is the oldest plutonic body of the Central Iberian Zone. Geotemas, 10, 249-252.
- Talavera, C., Montero, P., Martinez Poyatos, D., Williams, I.S., 2012. Ediacaran to Lower Ordovician age for rocks ascribed to the Schist–Graywacke Complex (Iberian Massif, Spain): Evidence from detrital zircon SHRIMP U–Pb geochronology. Gondwana Research, 22, 928-942.
- Talavera, C., Montero, P., Bea, F., Gonzalez Lodeiro, F., Whitehouse, M., 2013. U-Pb Zircon geochronology of the Cambro-Ordovician metagranites and metavolcanic rocks of central and NW Iberia. International Journal of Earth Sciences, 102(1), 1-23.
- Taylor, S.R., Emeleus, C.H., Exley, C.S., 1956. Some anomalous K/Rb ratios in igneous rocks and their petrological significance. Geochimica et Cosmochimica Acta, 10(4), 224-229.
- Teipel, U., Eichhorn, R., Loth, G., Rohrmuller, J., Holl, R., Kennedy, A., 2004. U-Pb SHRIMP and Nd isotopic data from the western Bohemian Massif (Bayerischer Wald, Germany): Implications for Upper Vendian and Lower Ordovician magmatism. International Journal of Earth Sciences, 93(5), 782-801.
- Valley, J.W., 2003. Oxygen isotopes in zircon. Reviews in mineralogy and geochemistry, 53(1), 343-385.
- Valverde-Vaquero, P., Dunning, G.R., 2000. New U-Pb ages for Early Ordovician magmatism in Central Spain. Journal of the Geological Society, 157, 15-26.
- Vervoort, J.D., Kemp, A.I.S., 2016. Clarifying the zircon Hf isotope record of crust–mantle evolution. Chemical Geology, 425, 65-75.
- Vialette, Y., Casquet, C., Fúster, J.M., Ibarrola, E., Navidad, M., Peinado, M., Villaseca, C., 1987. Geochronological study of orthogneisses from the Sierra de Guadarrama (Spanish Central System). Neues Jahrbuch für Mineralogie Monatshefte, 10, 465-479.
- Wildberg, H.G., Bischoff, L., Baumann, A., 1989. U-Pb ages of zircons from meta-igneous and meta-sedimentary rocks of the Sierra de Guadarrama: Implications for the Central Iberia crustal evolution. Contributions to Mineralogy and Petrology, 103, 253-262.
- Williams, I.S., Claesson, S., 1987. Isotopic evidence for the Precambrian provenance and Caledonian metamorphism of high grade paragneisses from the Seve Nappes, Scandinavian Caledonides. II: Ion microprobe zircon U-Th-Pb. Contribution to Mineralogy and Petrology, 97, 205-217.

Manuscript received December 2016; revision accepted September 2017; published Online October 2017.

# **ELECTRONIC APPENDIX I**

## Supplementary material available at:

- -Table I: revistes.ub.edu/public/journals/13/article1/TableI.xlsx
- -Table II: revistes.ub.edu/public/journals/13/article1/TableII.xlsx
- -Table III: revistes.ub.edu/public/journals/13/article1/TableIII.xlsx
- $Table\ IV:\ revistes. ub. edu/public/journals/13/article 1/Table IV.xlsx$
- -Table V: revistes.ub.edu/public/journals/13/article1/TableV.xlsx